EUROPEAN ORGANIZATION FOR NUCLEAR RESEARCH

CERN-EP/89-52
11 April 1989

BEAM TEST OF AN IMAGING HIGH-DENSITY PROJECTION CHAMBER

P. Fonte[1], A. Breskin[2], G. Charpak[1], W. Dominik[3,1] and F. Sauli[1]

ABSTRACT

A beam test of a High-Density Projection Chamber with optical readout is presented. The device consists of a prototype of the DELPHI HPC calorimeter on which a parallel-plate, light-emitting structure was installed, replacing the original multiwire proportional chamber readout system. It produces detailed images of the energy deposited by electromagnetic showers; hadronic interactions are easily discriminated from these. The computerized readout system gives full quantitative information on the events, showing good energy and position resolutions.

Paper presented by P. Fonte at the
Wire Chamber Conference,
Vienna, 13–17 February 1989

---

1) CERN, Geneva, Switzerland.
2) Weizmann Institute, Rehovot, Israel.
3) On leave of absence from the Institute of Experimental Physics, University of Warsaw, Poland.

1. INTRODUCTION

The detector described in this paper is an optical readout calorimeter, which we call an Imaging High-Density Projection Chamber (IHPC). It consists of a high-density drift volume [1], terminating in an imaging chamber [2–6]. The images of the events are detected by an intensified charge-coupled device (CCD) camera.

We performed a beam test with this device in order to investigate the ability of imaging chambers to detect electromagnetic showers and hadronic interactions. We also benefited from the high granularity of the device (about 30,000 pixels) to get a detailed view of the event structure in a gas sampling calorimeter. With further analysis, we will attempt to improve the calorimetric measurements by using statistical information eventually contained in the shower topology.

In this paper the test is described and the first quantitative results on basic parameters are presented. Early results with a small prototype of this kind were presented in Ref. [5].

2. THE DETECTOR

The high-density drift volume (called the '1 mm prototype'), where the showers develop, was built by the CERN DELPHI HPC Group using the 'lead-wire ribbon' technique [7] (see fig. 1). Its dimensions are $60 \times 44 \times 27$ cm^3, presenting 10.5 radiation lengths (X_0) and 0.34 interaction lengths to the incoming particles (along the 44 cm side), and it contains about 110 kg of lead. The 40 gas gaps sample the showers at intervals of $0.25X_0$.

Ionization electrons, created in the gas gaps by charged particles in the electromagnetic shower, drift towards a parallel-plate chamber where they are amplified. Charge multiplication occurs between two parallel meshes, 9 mm apart. The drift-time over the 27 cm long region is 8.2 μs, with a drift field of 600 V/cm. The gas mixture used [argon + triethylamine (TEA) vapour at 5 °C (95%) and CH_4 (5%)] fluoresces under the impact of the electrons in the avalanches, emitting UV light [8, 9]. This light is proximity-focused onto a thin sheet of plastic wavelength shifter*), placed in contact with the upper mesh of the amplifying gap. This converts the UV light to visible violet light, peaked at 420 nm—the region of highest sensitivity for many photocathodes, and of full transparency for standard optics (windows, lenses, etc.). The volume is closed by a double window of Mylar, with a flow of pure argon in between.

The events are imaged by an intensified CCD camera**) constructed from a gateable microchannel-plate image intensifier, an active image taper, and a CCD having 208×144 pixels (details of the camera are given in Ref. [10]). The 208 pixels were imaged along the 44 cm side of the detector (longitudinal beam direction), yielding a granularity of 2.1 mm per pixel. Along the transverse beam direction, the granularity is 2.3 mm per pixel, covering 33 cm. The driver electronics for the CCD provides a standard video signal that can be fed into standard video equipment.

3. THE TEST SET-UP

The detector was installed in a unseparated beam, composed mainly of pions and electrons, at the CERN Proton Synchrotron (PS) East Hall facility. Two threshold Cherenkov counters provided e/π discrimination on the level of 99% efficiency. A narrow beam in the transverse plane was defined by triggering on a 2 mm wide scintillator, placed vertically. The allowed vertical beam size was 2 cm, and the angular aperture of the beam is geometrically bound to be $\leq$ 10 mrad.

---

*) Courtesy of M. Bourdinaud, Saclay.

**) Designed and assembled by J. Dupont and J.-P. Fabre, Experimental Facilities Division, CERN.

Owing to the natural alpha radioactivity of the lead in the converter (which induces sparking), the amplifying gap had to be kept at a reduced gain, and a square pulse of 1.2 kV and 10 μs width was applied whenever the full gain was required in order to detect an event. The pulse height chosen was such that the chamber still operates in proportional mode, the readout being completely insensitive to any electronic noise induced by this pulse. A 10 μs gate pulse was also applied to open the image intensifier in front of the CCD, thus avoiding any light-noise that would be superimposed on the event during the 20 ms CCD integration time.

A photomultiplier (PM) assembled near the CCD camera gave a time-discriminated signal proportional to the total light coming from the successive horizontal layers of the drift volume, thus providing information about the shower development in depth. Using this depth-discriminated information and a beam of cosmic muons crossing the chamber along the drift direction, the drift attenuation was measured to be 50% after the maximum drift length of 27 cm.

The video signal was read by a MATROX-VIP640 VME-bus image digitizer having an accuracy of 8 bits in a 512 $\times$ 128 matrix (thus losing 16 CCD lines). For the PM, a LeCroy-ICA2261 CAMAC module provided 10-bit resolution on 320 channels sampled at 30.4 ns intervals (equivalent to 1 mm per channel because the last 50 buckets lie outside the drift-time). The data-acquisition system (CERN-VALET-PLUS VME-bus microcomputer and CAMAC) allowed a maximum of four events per spill to be recorded on tape, the event size being 66 Kbytes.

Examples of an 8 GeV/c electromagnetic shower and a 5 GeV/c pion (or proton interaction can be seen in figs. 2 and 3, respectively; their obvious difference implies that the e/π identification may be very good. These pictures lose much of their quality in the printing process, compared with the beautiful high-resolution colour-coded pictures that can be seen with a video monitor.

4. FIRST RESULTS

The energy resolution of the IHPC for electromagnetic showers (fig. 4) was calculated either from the PM or from CCD signals. The CCD signal, forming an image, gives information about the image content (total light) and also about the image surface. The image surface is calculated by counting the number of pixels above the pedestal-subtracting threshold, the sum being considered as a measure of the energy. The image content is the sum of all pixel values after pedestal subtraction.

At 5 and 8 GeV the energy resolution from the image content and the PM (total light) is comparable with the values measured by the DELPHI Group in the same converter with a multiwire proportional chamber (MWPC) readout [11]. The poorer resolution of the IHPC at 2 GeV is attributable to a lack of gain in the single amplifying gap. In fact, a separate run with a 30% superior gain yielded a resolution of 18% at 2 GeV instead of the 20% presented. The PM and CCD readouts show strictly the same behaviour. It is clear that a short converter such as this one will not follow a $1/\sqrt{E}$ law; a deviation from the $14\%/\sqrt{E}$ law followed by the points at lowest energy is already visible at 2 GeV for the DELPHI data (see ref. [7]). For all energies, but particularly for low energy, the image surface provides a better resolution (13% at 2 GeV) than does the total light (20% at 2 GeV). In all cases the resolution is sharply degraded by any increase in the pedestal-subtracting threshold.

The signals from the CCD and the PM are highly correlated, as can be seen in fig. 5a, the clusters from 2, 5, and 8 GeV events being clearly separated. Their centroids are marked with a cross. In fig. 5b, a scatter plot of the image content versus image surface is shown. The image-surface data show a tendency to saturate at higher energies—a tendency probably worsened by the non-containment of the showers.

In order to reconstruct the projection of the line of flight of the incident particle on the image plane (shower axis), the following procedure was used:

i) the centroids of every pixel row perpendicular to the shower axis were calculated and their dispersion (σ) about the average was calculated for the 5 GeV data;

ii) the calculated dispersions were used to weight a linear least-squares fit to the pixel-row centroids for every event, yielding the angle and the impact coordinate;

iii) all the lines were superimposed for the 5 GeV data, and the point of smaller transverse dispersion was defined as the reference plane for the position measurement. A particle position is thus defined as the intersection of the axis with the reference plane. This plane lies at $4.1X_0$ and was used for all energies. It does not change significantly from 2 to 8 GeV.

Other procedures, such as using the weighted mean of all centres of gravity to estimate the impact point, or using variable weights for every row, proportional to the total light in the row, produced worse results.

The results from the procedure we used can be seen in figs. 6a and 6b. The angular resolution (σ_θ) is about 32 mrad at 8 GeV and seems to follow an 83 mrad/$\sqrt{E}$ law in the energy range studied. This angular resolution is worse by about a factor of 2 than the value of 38 mrad obtained by the DELPHI group [7] at 1 GeV. A possible reason for this might be the purely two-dimensional nature of the information in the IHPC image, compared with the three-dimensional information of the DELPHI HPC.

A position resolution of 9.8 mm/$\sqrt{E}$ (fig. 6b) can be compared with the resolutions achieved by using MWPC techniques for shower sampling [12, 13]. The effects of the beam dispersion for both the angular and the position resolution measurements lie within the error bars.

A contour plot of an average of 400 shower images at 8 GeV is shown in fig. 7. The shower broadens in the first $4X_0$, after which it keeps essentially the same width up to $9X_0$. Concentric contours over the central axis mark the centres of the gas gaps. This figure clearly shows that the showers are not contained. In fig. 8 the transverse image profile of the average of 8 GeV shower images is plotted for 2, 6, and 9 radiation lengths. The two indentations on each side of the peak correspond to mechanical supports inside the drift volume (dead zones).

5. CONCLUSIONS

The beam test of an Imaging High-Density Projection Chamber in the energy range from 2 to 8 GeV shows that the characteristics of the device seem to be close to those obtained with conventional MWPC readout for the same converter (only $10.5X_0$): 20% energy resolution (σ_E/E) at 2 GeV; 9.8 mm/$\sqrt{E}$ position resolution; 83 mrad/$\sqrt{E}$ angular resolution. The high granularity offers the possibility to carry out some non-conventional analysis; for instance, by considering the total surface of the shower's image as a measure of the incident energy, the energy resolution is improved to 13% at 2 GeV. More elaborate algorithms, which rely on the fine detail of the images, are being studied for improved particle identification and increased accuracy of electromagnetic calorimetric measurements.

The IHPC shows promise in applications where the rare or complex phenomena being studied need a high data-redundancy (the cost per analog channel is remarkably low). Also, it may be suitable for covering large surfaces when the showers are still contained in a fairly big number of pixels.

Acknowledgements

We wish to thank O. Ullalland and H.G. Fischer for lending us the converter and for their assistance during the transformation work, and M. Bourdinaud for providing the wavelength shifter. The technical assistance of R. Bouclier, G. Million and J.C. Santiard was very much appreciated.

REFERENCES

[1] H.G. Fischer and O. Ullaland, IEEE Trans. Nucl. Sci. **NS-27** (1980) 78.

[2] R.S. Gilmore et al., Nucl. Instrum. Methods **206** (1983) 189.

[3] D.M. Potter, Nucl. Instrum. Methods **228** (1984) 56.

[4] T.K. Gooch et al., Nucl. Instrum. Methods **A241** (1985) 363.

[5] G. Charpak et al., Nucl. Instrum. Methods **A258** (1987) 177.

[6] G. Charpak et al., IEEE Trans. Nucl. Sci. **NS-35** (1988) 483.

[7] CERN-DELPHI 85-19 GEN-22 (1985).

[8] M. Suzuki et al., Nucl. Instrum. Methods **A254** (1987) 556.

[9] V. Peskov et al., preprint CERN-EP/88-167, submitted to Nucl. Instrum. Methods (1988).

[10] A. Breskin et al., Nucl. Instrum. Methods **A273** (1988) 798.

[11] H.B. Crawley et al., Test results from the 1 mm prototype at DESY, Iowa State University report, February 1985, unpublished.

[12] R. Bouclier et al., Nucl. Instrum. Methods **A267** (1988) 69.

[13] E. Gabathuler et al., Nucl. Instrum. Methods **157** (1978) 47.

Figure captions

Fig. 1 : Schematic view of the IHPC.

Fig. 2 : Example of an 8 GeV/c electromagnetic shower.

Fig. 3 : Example of a 5 GeV/c hadronic interaction.

Fig. 4 : Energy resolution. When the incident energy is estimated by the total light emitted by an event (photomultiplier and image content data), the IHPC energy resolution is comparable with the energy resolution measured in the same converter with MWPC readout (DELPHI HPC). If the image surface is considered as a measure of the energy, there is an improvement in the energy resolution, particularly at low energies. The image surface is calculated by counting the number of pixels above the pedestal-subtracting threshold, and the image content (total light) is calculated by summing all the pixel values after pedestal subtraction.
Key: ○ DELPHI HPC; * IHPC (image content); ▵ IHPC (image surface); □ IHPC (photomultiplier).

Fig. 5 : a) Photomultiplier versus image content (both quantities are converted to a GeV scale). The good correlation between these two independent forms of readout is evident.
b) Image surface versus image content (both quantities are converted to a GeV scale). The image surface grows more slowly than the image content (total light) with increasing incident energy.

Fig. 6 : a) Angular resolution: this follows an 83 mrad/$\sqrt{E}$ law.
b) Position resolution: fitted by 9.8 mm/$\sqrt{E}$.

Fig. 7 : Contour plot of an average of 8 GeV/c showers. The energy leakage through the end of the converter is clearly visible.

Fig. 8 : Transverse cuts on the average image of 8 GeV/c showers at 2, 6, and 9 radiation lengths. The two indentations (dead zones), are explained in the text.

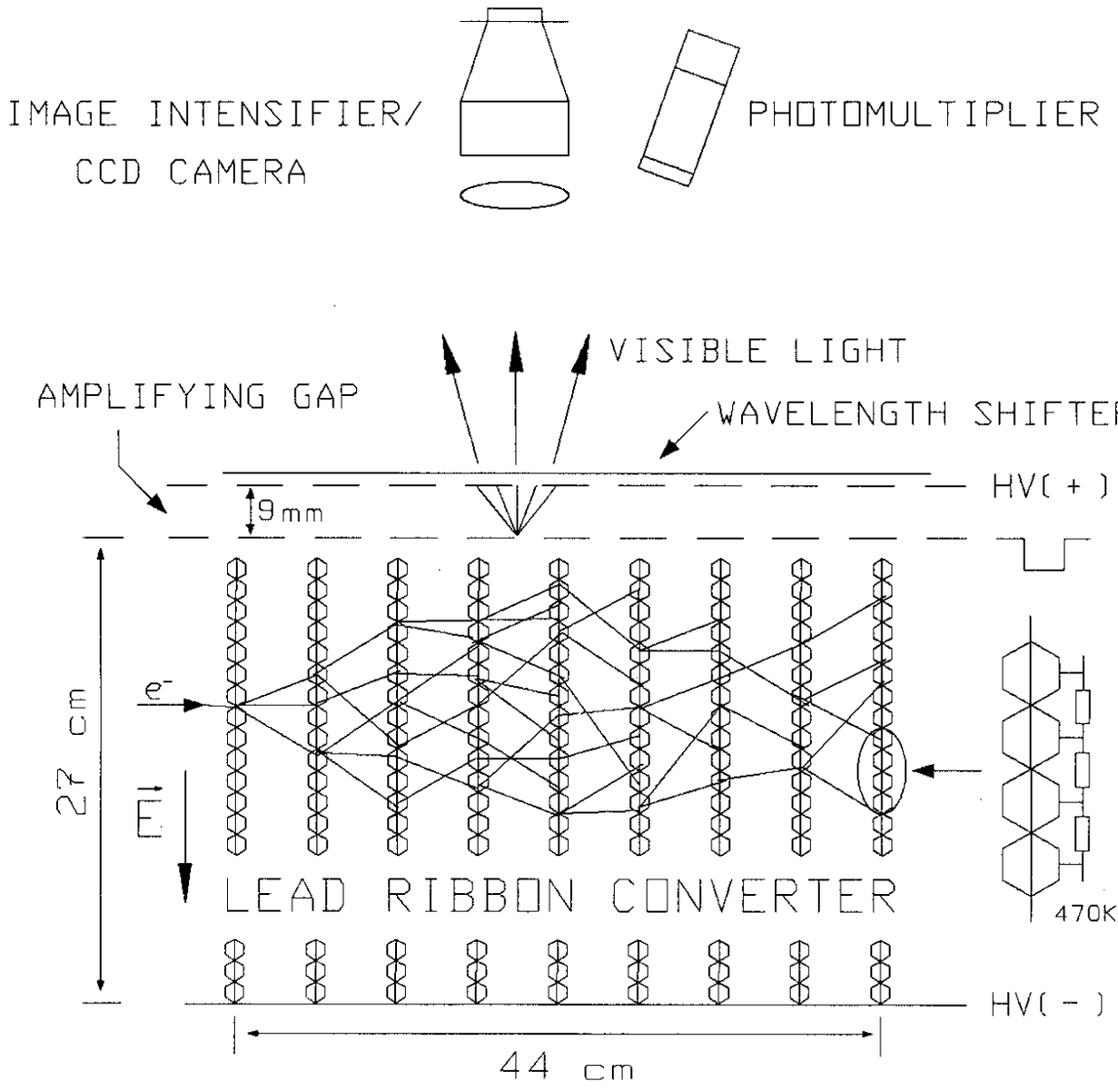
IMAGE INTENSIFIER/
CCD CAMERA
PHOTOMULTIPLIER
VISIBLE LIGHT
AMPLIFYING GAP
WAVELENGTH SHIFTER
HV(+)
9 mm
27 cm
e⁻
E
LEAD RIBBON CONVERTER
470K
HV(-)
44 cm

Fig. 1

Fig. 2

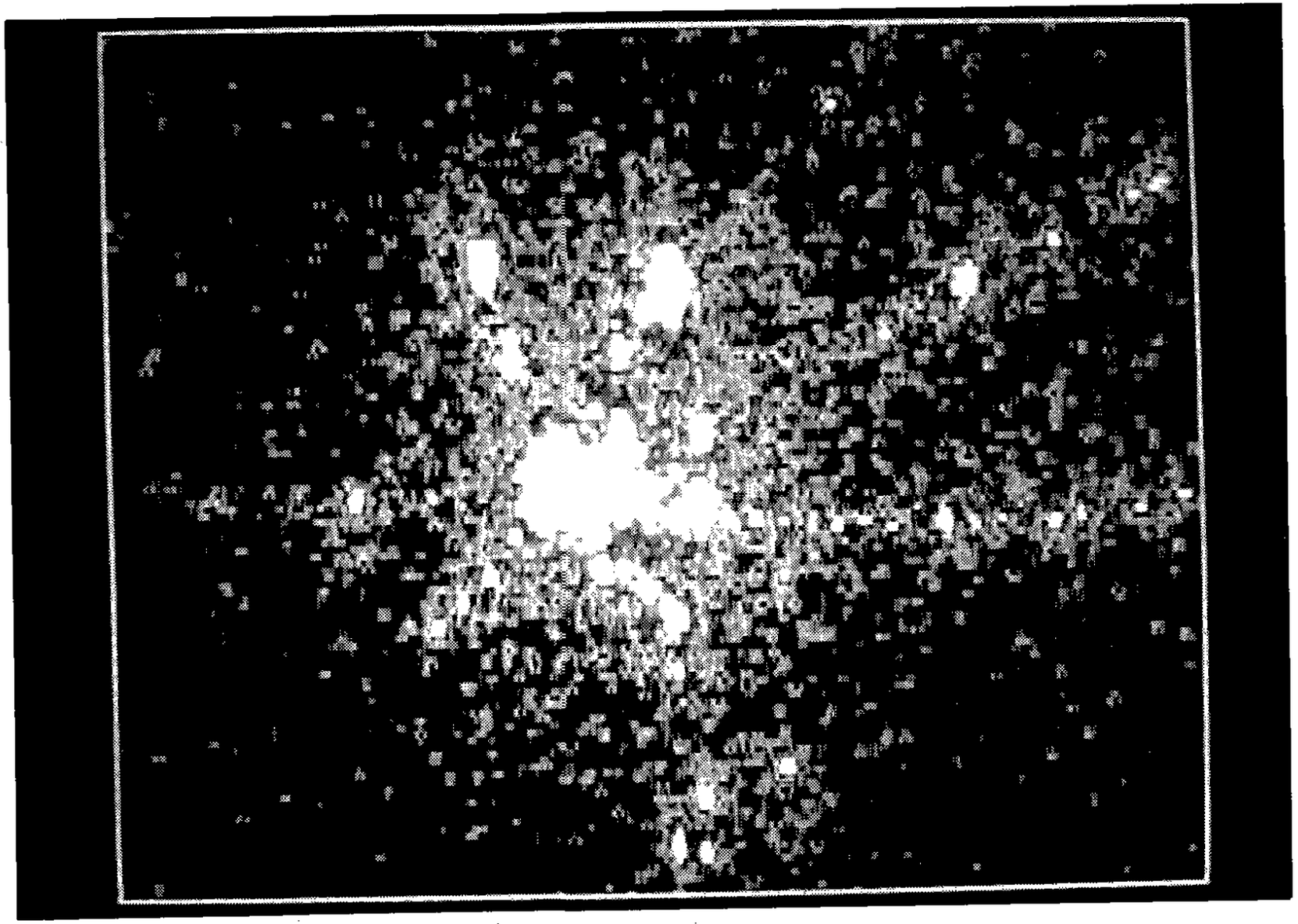

Fig. 3

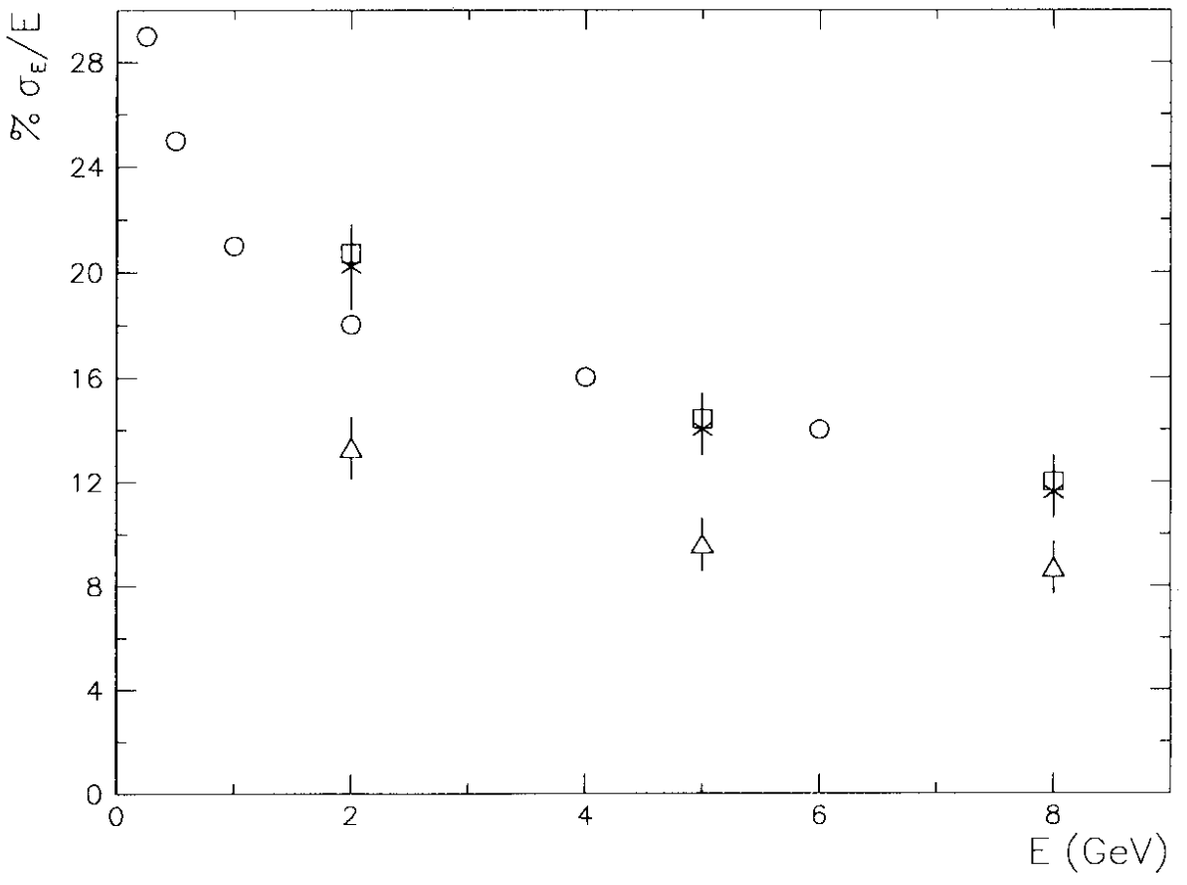

Fig. 4

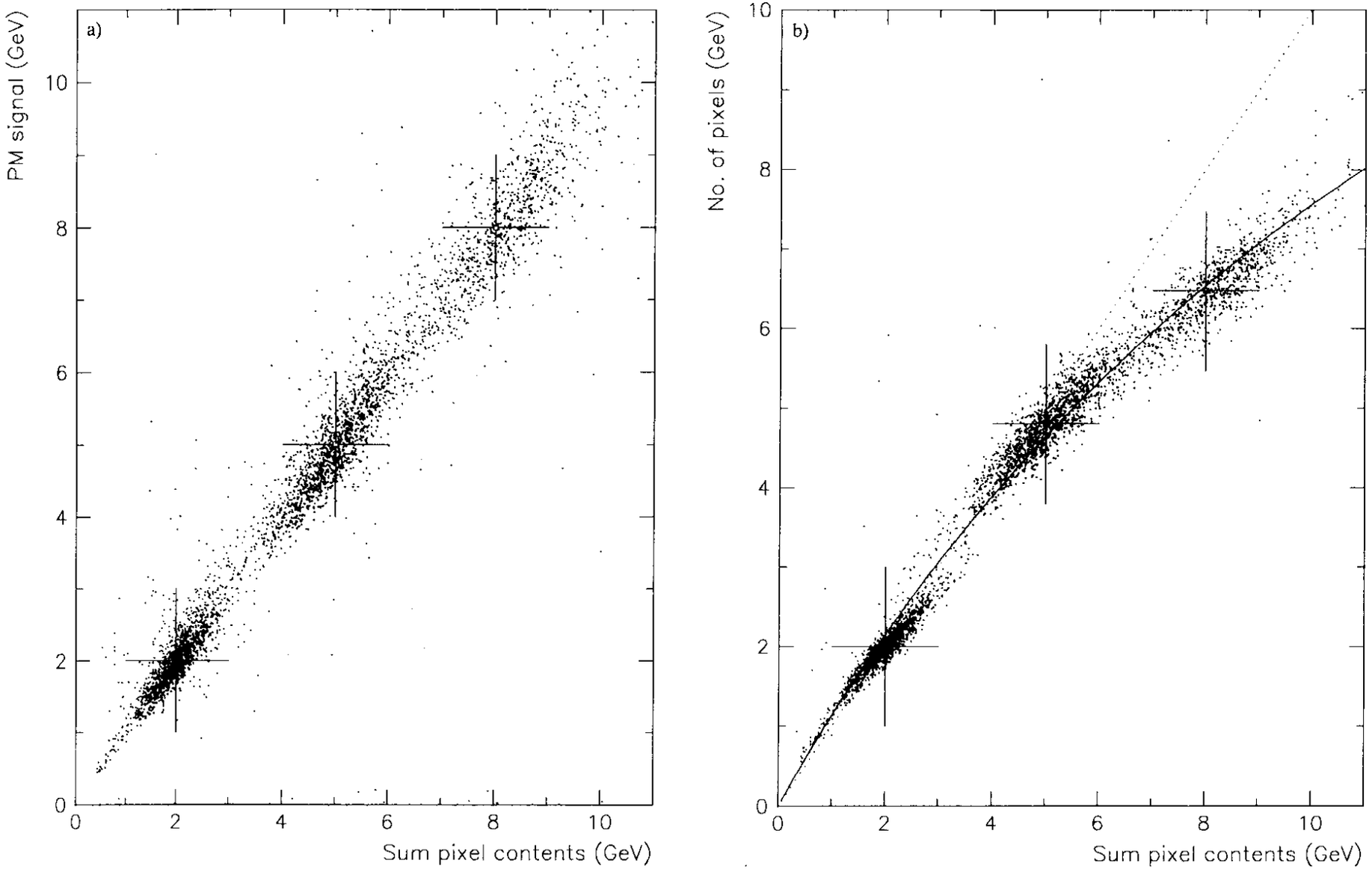
a)
PM signal (GeV)
Sum pixel contents (GeV)
b)
No. of pixels (GeV)
Sum pixel contents (GeV)

Fig. 5

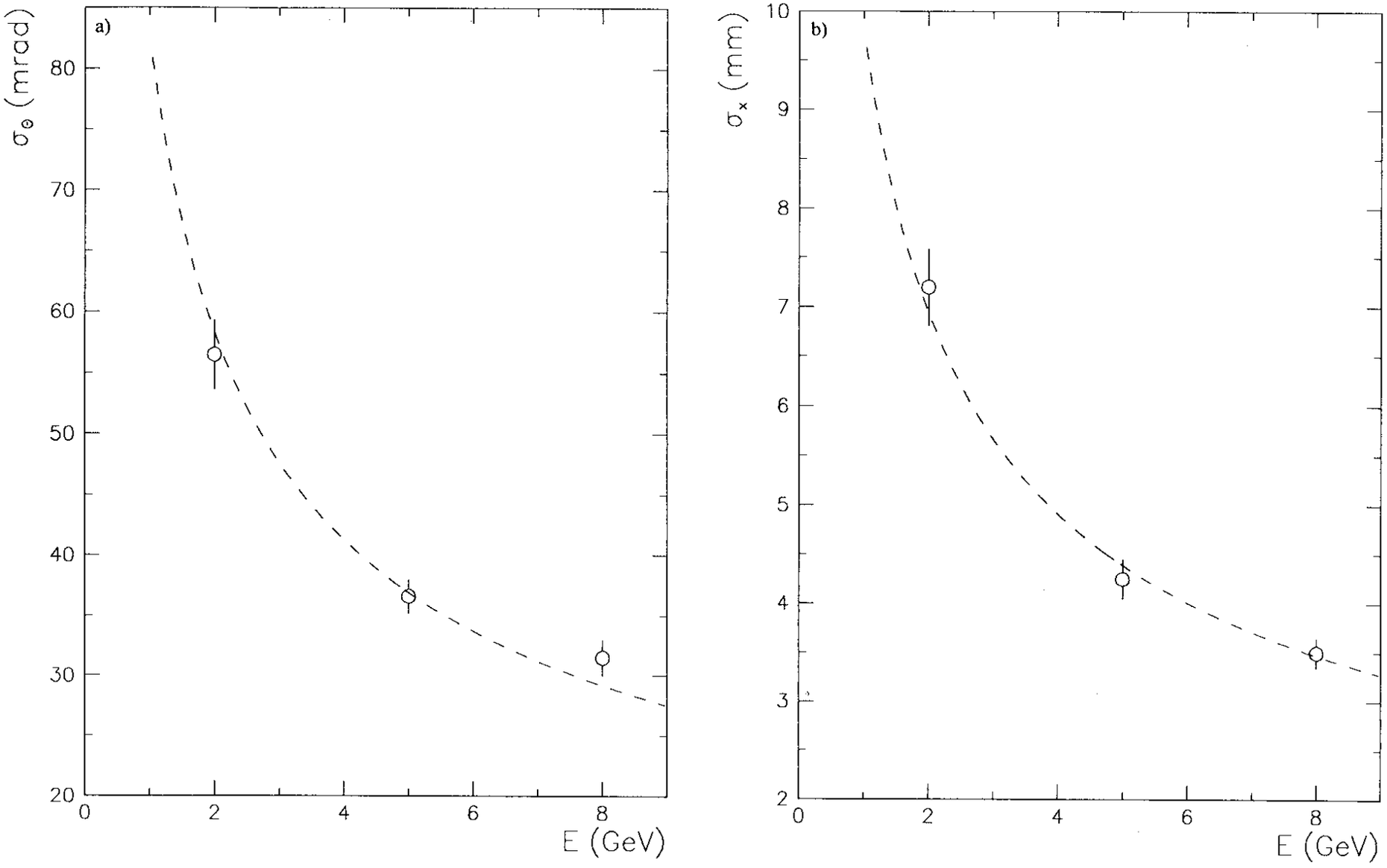
a)
σ_Θ (mrad)
80
70
60
50
40
30
20
0
2
4
6
8
E (GeV)
b)
σ_x (mm)
10
9
8
7
6
5
4
3
2
0
2
4
6
8
E (GeV)

Fig. 6

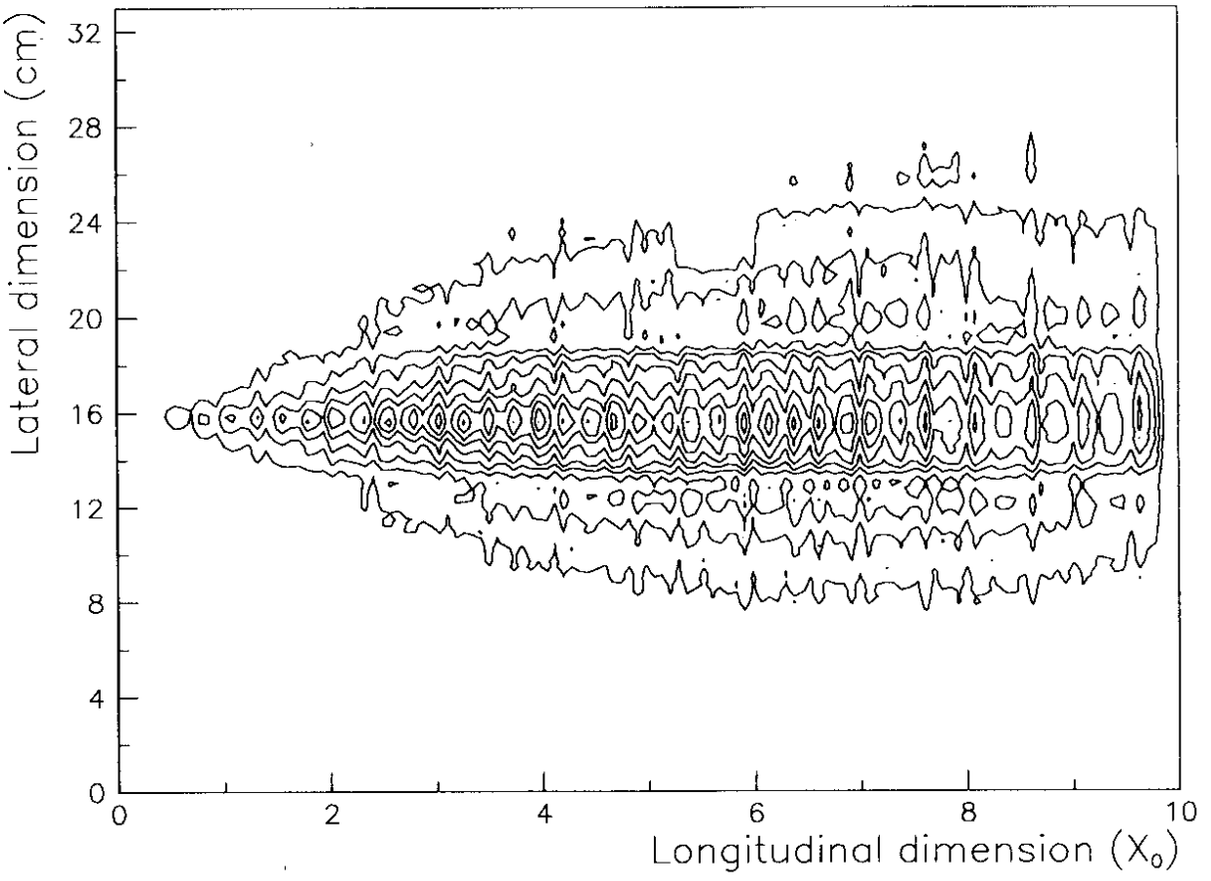
Lateral dimension (cm)
32
28
24
20
16
12
8
4
0
0
2
4
6
8
10
Longitudinal dimension (X_0)

Fig. 7

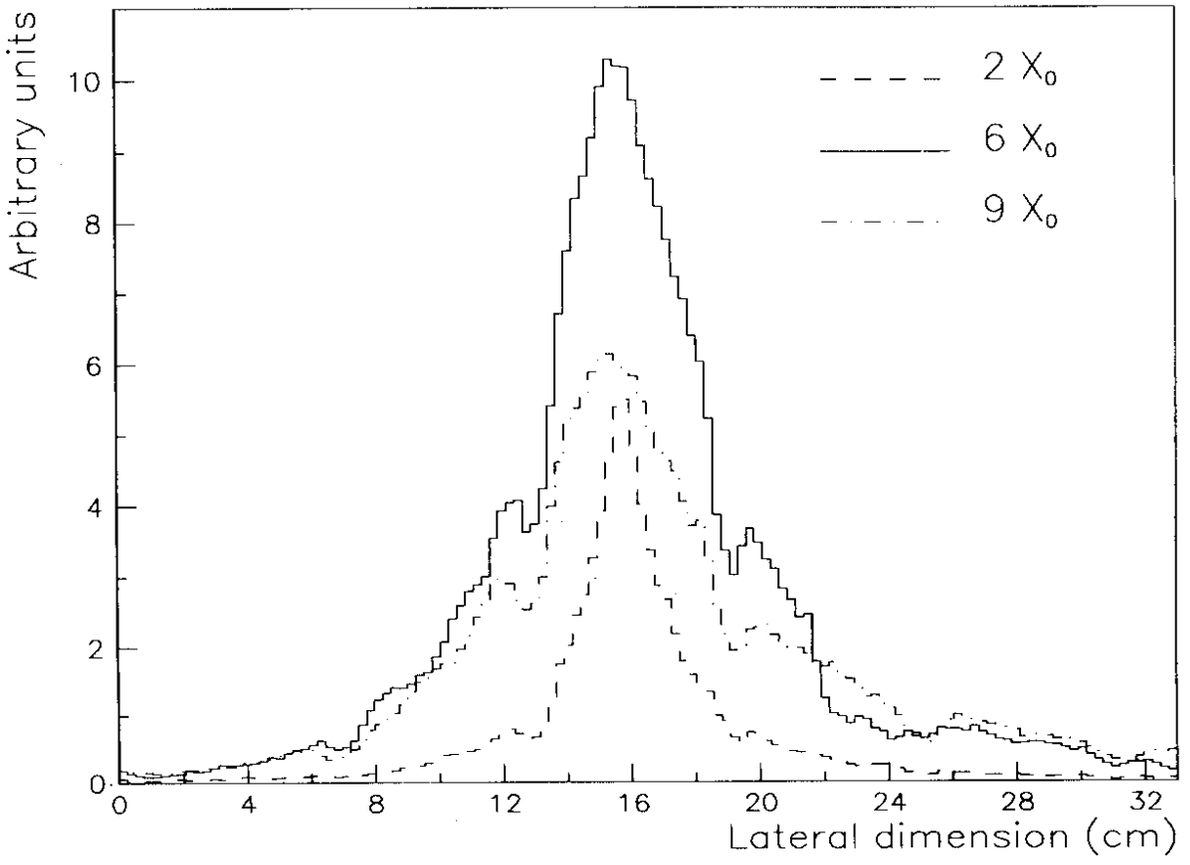
Arbitrary units
10
8
6
4
2
0
0
4
8
12
16
20
24
28
32
Lateral dimension (cm)
2 X_0
6 X_0
9 X_0

Fig. 8